

Contribution of galaxies to the background hydrogen-ionizing flux

Julien E. G. Devriendt,¹ Shiv K. Sethi,¹ Bruno Guiderdoni¹ and Biman B. Nath²

¹*Institut d'Astrophysique de Paris, CNRS, 98bis Boulevard Arago, F-75014 Paris, France*

²*Raman Research Institute, Bangalore-560080, India*

Accepted 1998 March 16. Received 1998 February 20; in original form 1997 November 28

ABSTRACT

We estimate the evolution of the contribution of galaxies to the cosmic background flux at 912 Å by means of a semi-analytic model of galaxy formation and evolution. Such modelling has been quite successful in reproducing the optical properties of galaxies. We assume that high-redshift damped Lyman α systems are the progenitors of present-day galaxies, and we design a series of models that are consistent with the evolution of cosmic comoving emissivities in the available near-infrared, optical, ultraviolet and far-infrared bands along with the evolution of the neutral hydrogen content and average metallicity of damped Lyman α systems. We use these models to compute the galactic contribution to the Lyman-limit emissivity and background flux for $0 \approx z \leq 4$. We take into account the absorption of Lyman-limit photons by H I and dust in the interstellar medium of the galaxies. We find that the background Lyman-limit flux due to galaxies might dominate (or be comparable to) the contribution from quasars at almost all redshifts if the absorption by H I in the interstellar medium is neglected. Such H I absorption would result in a severe diminishing of this flux – by almost three orders of magnitude at high redshifts and by one to two orders at $z \approx 0$. Though the resulting galaxy flux is completely negligible at high redshifts, it is comparable to the quasar flux at $z \approx 0$.

Key words: methods: analytical – dust, extinction – galaxies: evolution – galaxies: fundamental parameters – cosmology: theory.

1 INTRODUCTION

The study of the evolution of the ionization state of the diffuse intergalactic medium (IGM) is crucial to understanding the formation of structures in the Universe. An important input into this study is the intensity and evolution of the background hydrogen-ionizing flux. The Universe is observed to be highly ionized at high redshifts (Gunn & Peterson 1965; Giallongo et al. 1994) and it is widely believed that the main mechanism of ionization is photoionization by photons at and below the Lyman limit. This view is borne out by estimates of background hydrogen-ionizing flux as inferred by the ‘proximity effect’, which fixes the value of this flux, $J_{\text{ion}} \approx 10^{-21 \pm 0.5} \text{ erg s}^{-1} \text{ cm}^{-2} \text{ Hz}^{-1} \text{ sr}^{-1}$ (Bajtlik, Duncan & Ostriker 1988; Bechtold 1994; Giallongo et al. 1996; Cooke, Espey & Carswell 1997) for $2 \lesssim z \lesssim 4.5$. It is not clear whether the observed quasars can provide sufficient contribution to the flux implied by this effect at $z \geq 3$ (Miralda-Escudé & Ostriker 1990; Giroux & Shapiro 1996; Haardt & Madau 1996; Cooke et al. 1997). In light of this fact, it was speculated that high-redshift star-forming galaxies could be the dominant contributor to this background flux (Songaila, Cowie & Lilly 1990). At smaller redshifts, there is a greater uncertainty in the level of this flux (Kulkarni & Fall 1993; Maloney 1993; Vogel et al. 1995; Reynolds et al. 1995); however, a

tight upper limit of $J_{\text{ion}} < 8 \times 10^{-23} \text{ erg s}^{-1} \text{ cm}^{-2} \text{ Hz}^{-1} \text{ sr}^{-1}$ at $z \approx 0$ exists from H α observations (Vogel et al. 1995). If this flux is entirely due to the background hydrogen-ionizing photons, then the contribution of quasars falls short of the observed value by nearly an order of magnitude at $z \approx 0$ (Madau 1992; Haardt & Madau 1996).

Recent years have seen tremendous progress in understanding the formation and evolution of galaxies at moderate and high redshifts. Prominent observations that made it possible are the probing of the evolution of galaxies with $z \leq 1$ by the Canada–France Redshift Survey (CFRS) (Lilly et al. 1995), the discovery of high-redshift galaxies using the ultraviolet (UV) drop-out technique (Steidel et al. 1996) in the *Hubble Deep Field* (HDF) (Madau et al. 1996; Sawicki, Lin & Yee 1997; Connolly et al. 1997), and a better understanding of the evolution of the neutral hydrogen content and average metallicity of damped Lyman α (DLA) systems from $z \approx 0$ to $z \approx 4$ (Lanzetta et al. 1995; Pettini et al. 1997). Several theoretical attempts have been made to explain these observations (Madau 1997a, b; Fall, Charlot & Pei 1996; Frenk et al. 1996; Guiderdoni et al. 1998, hereafter GHBM). These observations give valuable clues about the history of star formation and the comoving emissivity in several wavebands in the Universe up to $z \approx 4$ and have provided a unique opportunity to model and study the contribution of star-forming galaxies to the background hydrogen-ionizing flux [for

recent attempts to estimate the hydrogen-ionizing flux from star-forming galaxies for $z \leq 1.5$ see Giallongo, Fontana & Madau (1997) and Deharveng et al. (1997)].

The CFRS observations give the evolution of cosmic emissivity at $\lambda \approx 2800 \text{ \AA}$ (in the rest frame of the emitter) for $z \leq 1$ while the HDF observations estimate the emissivity at $\lambda \approx 1620 \text{ \AA}$ for $2.5 \leq z \leq 4$. Our aim in this paper is to extrapolate the results from these important UV wavelengths to calculate the emissivity (and background flux) at the Lyman-limit wavelength. The hydrogen-ionizing photons are emitted by massive stars with lifetimes $\approx 10^7 \text{ yr}$, so their flux is not sensitive to the history of galaxy evolution, which has much larger time-scales. Conversely, one can view it as a direct measurement of the instantaneous star formation rate (SFR). The conversion of emissivity from the wavelengths probed by HDF and CFRS to 912 \AA requires knowledge of three factors:

- (i) the absorption of photons with $\lambda \leq 912 \text{ \AA}$ within the stellar atmosphere;
- (ii) the amount of dust and the spectral index of dust absorption coefficient in the interstellar medium;
- (iii) the amount of neutral hydrogen in the interstellar medium.

The first factor is fixed by stellar atmosphere models and depends mainly on the choice of initial mass function (IMF), which is guided by our ability to reproduce observed colours of galaxies.

In extrapolating the amount of dust absorption from the observed value at 1620 \AA (or 2800 \AA) to the Lyman-limit wavelength, it is important to know the amount of dust in galaxies as accurately as possible, because $A_{912}/A_V \approx 5$ as compared to $A_{1600}/A_V \approx 2.5$. Therefore a small uncertainty in the dust extinction at UV wavelengths translates into a much larger error in the extinction at the Lyman limit. We can use available far-infrared (FIR) data to fix the amount of dust at $z \approx 0$. At higher redshift, we can fix it by matching the observed average metallicity of DLA absorbers (Pettini et al. 1997) and by reproducing the cosmic infrared background (CIB) reported by Puget et al. (1996).

The most crucial factor in determining the absorption of hydrogen-ionizing photons in the interstellar medium (ISM) is the amount of H I and its distribution in galaxies. We can model this by using the available data on DLA absorbers, which give the evolution of the average H I content of these clouds for $0 \leq z \leq 4$ (Lanzetta et al. 1995). In our study we have to assume that DLA absorbers belong to the same population of galaxies as the ones that are observed in emission in the CFRS and HDF. No clear consensus has been reached on this point yet, but recent observations may support the explanation that the DLA absorbers are either thick rotating discs or protogalactic clumps (Haehnelt, Steinmetz & Rauch 1997; Prochaska & Wolfe 1997). Thereafter we assume the H I, dust and stars to be homogeneously distributed in the ISM. This assumption gives the maximum possible H I absorption and allows us to obtain a lower limit on the fraction of Lyman-limit photons escaping from the galaxies. We shall also briefly discuss the implications of the clumpiness of H I.

We use a semi-analytic model of galaxy formation to study the evolution of background hydrogen-ionizing flux for $0 \approx z \leq 4$ (for details see e.g. GHBM). In Section 2, we describe the relevant features of this model and its various assumptions. The basic method of obtaining the background ionizing flux given the comoving emissivity and various sources of intergalactic absorption is also briefly described in this section. Our results are detailed in Section 3. In Section 4 we discuss various uncertainties and possible improvements in our estimates, and summarize our conclusions in Section 5.

2 SEMI-ANALYTIC MODELS AND HYDROGEN-IONIZING FLUX

We do not attempt to give a detailed description of semi-analytic models of galaxy formation and evolution. Readers interested in details are referred to a recent paper (GHBM and references therein). We just introduce and define the parameters required for our work.

2.1 Collapse of haloes and cooling

We consider fluctuations in the matter density distribution at high redshift to be spherically symmetric ('top hat' approximation, see e.g. Peebles 1980) on galactic scales. As a result of the violent relaxation process that they undergo after collapsing at redshift z_{coll} , such haloes virialize. One can then use the peaks formalism (Bardeen et al. 1986) to compute the mass distribution of such haloes, as in Lacey & Silk (1991) and Lacey et al. (1993), for a given cosmological model.

The baryonic gas subsequently radiates away its energy, falling deeper and deeper in the potential well, until it reaches rotational equilibrium and settles into a disc-like structure. Thus, the length scale r_{disc} of the cold gas exponential disc can be inferred from the initial radius r_v by conservation of angular momentum, $r_{\text{disc}} \approx \lambda_J r_v$, where λ_J is the dimensionless spin parameter (Fall & Efstathiou 1980). Only discs can form in this formalism. The formation of elliptical galaxies (and of bulges of spiral galaxies) has to be explained by the merging of discs. Kauffmann, White & Guiderdoni (1993) and Cole et al. (1994) showed that this process can explain the current fraction of giant ellipticals among bright galaxies.

2.2 Star formation

It is well known that local physical processes governing star formation are complex and depend on various parameters. Nevertheless, it seems that, on galaxy scales, one can phenomenologically define a mean SFR per unit surface density, which is proportional to the total gas surface density (neutral plus molecular) divided by the dynamical time-scale of the disc (Kennicutt 1989, 1997). Hence we assume that the star formation time-scale t_* is proportional to the dynamical time-scale of the disc: $t_* \equiv \beta(z)t_{\text{dyn}}$, where $t_{\text{dyn}} \equiv 2\pi r_{\text{disc}}/V_c$. In the previous formula $V_c = (GM/r_v)^{1/2}$ is the circular velocity of the dark matter halo of mass M , and $\beta(z)$ is our first free parameter, which we allow to vary with redshift in order to reproduce the shape of the cosmic comoving emissivity at 1620 and 2800 \AA from $z = 0$ to $z = 4$. The SFR at time t is then computed as follows:

$$\text{SFR}(t) = \frac{M_{\text{gas}}(t)}{t_*}. \quad (1)$$

As shown in GHBM (their fig. 3), using such a prescription allows one to match the average value and width of the observed distribution of 'Roberts time' for a sample of $z \approx 0$ bright disc galaxies given by Kennicutt, Tamblyn & Congdon (1994), just by taking $\beta(0) \approx 100$. Furthermore, as pointed out by these authors, the shape of the cosmic comoving SFR density curve (their fig. 9) suggests a strong evolution of β with redshift. Our model shares the same spirit: we consider the star formation history in the Universe as a sum of contributions from a population of quiescent star-forming galaxies and a population of starburst galaxies whose respective proportions are modelled through $\beta(z)$. We allow $\beta(z)$ to vary from ≈ 0.5 to ≈ 200 , which respectively correspond to starburst and quiescent mode of star formation.

2.3 Stellar feedback

Stellar feedback is modelled following the original work by Dekel & Silk (1986). It stems from massive star explosions, which expel gas from the galaxies, preventing further star formation from occurring. Physically, when the thermal energy ejected by supernovae becomes greater than the binding energy of the halo, one expects such winds to be triggered with a certain efficiency. One can then compute the mass fraction of stars forming before the galactic wind:

$$F_* \equiv \frac{M_*}{(M_* + M_{\text{gas}})} = [1 + (V_{\text{hot}}/V_c)^\alpha]^{-1}, \quad (2)$$

where V_{hot} and α are obtained through a fit based on Smoothed Particle Hydrodynamics simulations of galaxy formation in which most of the feedback effect is due to momentum exchange as in Cole et al. (1994). But one should bear in mind that there is much uncertainty on these parameters mostly because of the treatment of supernova remnant interactions with the ISM. Moreover, as pointed out by Efstathiou (1992) and Blanchard, Valls-Gabaud & Mamon (1992), there is likely to be an overall high- z reheating of the intergalactic medium, which could prevent cooling in haloes with circular velocities below $V_c \sim 20\text{--}50 \text{ km s}^{-1}$, and possibly as high as $\sim(200)^{1/3}V_c$ in the case of adiabatic collapse. To sum up, the situation is very complicated because we lack a global theory of feedback processes. Therefore, we adopt a rather crude but simple approach to the problem: we do not attempt to model the redshift dependence of local or global feedback in this paper, but we just consider the values derived from numerical simulations for a typical 10 per cent feedback efficiency of momentum exchange. They give $\alpha = 5$ and $V_{\text{hot}} = 130 \text{ km s}^{-1}$. In the following, we keep the same value for α and allow our second free parameter, V_{hot} , to vary between 100 and 130 km s^{-1} .

2.4 Stellar populations

We use a coupled model of spectrophotometric and chemical evolution in order to compute the age dependence and metallicity of the gas content and of the UV to near-infrared (NIR) spectra of the stellar populations in a self-consistent way. The end-product of these models are time-dependent synthetic spectra and gas/metallicity evolution of galaxies. The model that is used here is based upon a new numerical scheme (isochrone), as well as on up-graded Geneva stellar tracks and yields, and will be described in Devriendt, Guiderdoni & Sadat (in preparation). The photometric properties of galaxies, which are our main interest in this study, are obtained after taking into account the intrinsic extinction caused by both neutral hydrogen absorption below 912 Å and dust (see following section).

2.5 Dust and gas absorption

Some of the energy released by stars in the UV and optical is absorbed by dust and H I gas (for wavelengths shorter than 912 Å) and re-emitted in the IR and submillimetre ranges. We would like to emphasize the difficulty of estimating these absorption processes since one has to address the complicated and crucial issue of the geometrical distribution of dust and gas relative to stars. In the following, we assume that the gas is distributed in an exponential disc with mean H I column density at time t ,

$$\langle N_{\text{HI,ISM}}(t) \rangle = M_{\text{gas}}(t)/1.4m_{\text{H}}\pi r_{\text{g}}^2, \quad (3)$$

where $r_{\text{g}} \equiv f_c r_{\text{disc}}$ is the truncation radius of the gaseous disc, f_c

being our third free parameter. The factor 1.4 accounts for the presence of helium. The mean optical thickness inside r_{g} is given by

$$\langle \tau_\lambda(t) \rangle = \left(\frac{A_\lambda}{A_V} \right)_{Z_\odot} \left(\frac{Z_{\text{g}}(t)}{Z_\odot} \right)^s \left(\frac{\langle N_{\text{HI,ISM}}(t) \rangle}{2.1 \times 10^{21} \text{ at cm}^{-2}} \right) + \langle N_{\text{HI,ISM}}(t) \rangle \sigma_{\text{HI}} \left(\frac{\lambda}{912 \text{ Å}} \right)^3 \Theta(912 \text{ Å}). \quad (4)$$

The first term contains: (i) the extinction curve for solar metallicity as measured by Mathis, Mezger & Panagia (1983); and (ii) the gas metallicity ($Z_{\text{g}}(t)$) dependence of the extinction curve, which is modelled as in Guiderdoni & Rocca-Volmerange (1987) and Franceschini et al. (1991, 1994), according to power-law interpolations based on the Solar Neighbourhood and the Magellanic Clouds, with $s = 1.35$ for $\lambda < 2000 \text{ Å}$ and $s = 1.6$ for $\lambda > 2000 \text{ Å}$. The second term is due to hydrogen absorption and hence is only used for wavelengths shorter than 912 Å (Θ being the Heaviside function); $\sigma_{\text{HI}} = 6.3 \times 10^{-18} \text{ cm}^2$ is the hydrogen ionization cross-section at the threshold.

Light scattering by dust grains is also modelled and the final optical depth is averaged over inclination angle, assuming that stars, dust and gas are homogeneously mixed as in Dwek & Városi (1996). These authors extended the radiative transfer calculation in a spherically symmetric ISM to the case of an ellipsoid, which is more relevant for our study. The results are quite similar to those obtained with a classic ‘slab’ geometry where stars, dust and gas are distributed with the same scaleheight, and seem to satisfy the estimates of extinction given by Andreani & Franceschini (1996). As the galaxy is optically thick to Lyman-limit photons, this homogeneous distribution of stars and dust implies that only a tiny fraction ($\approx 1/\langle \tau_{912} \rangle$) of Lyman-limit photons will be able to escape from the galaxy: the ones emitted by stars located in a thin outer shell (with column density $\approx 1/\sigma_{\text{HI}} \approx 1.6 \times 10^{17} \text{ at cm}^{-2}$) of the gaseous disc. This procedure enables one to compute the bolometric luminosity absorbed by dust and reprocessed in the IR/submillimetre range.

2.6 Dust emission

Here, we will not give details on how we derive the IR/submillimetre spectrum (see GHBM), but just briefly outline the steps that lead to the emission spectrum. As mentioned in the previous section, we compute the optical depth of the discs, and the amount of bolometric luminosity absorbed by dust. The last step consists of the computation of emission spectra of galaxies in the IR/submillimetre wavelength bands. This is completed by using a three-component dust model (polycyclic aromatic hydrocarbons, very small grains, and big grains), which is described in Désert, Boulanger & Puget (1990). The method employed is very similar to that developed by Maffei (1994), and is based upon observational correlations (see Soifer & Neugebauer 1991) of the *IRAS* flux ratios with the total IR luminosity (Devriendt et al., in preparation).

2.7 Hydrogen-ionizing flux

Once one has computed the fraction of hydrogen-ionizing photons that effectively escape from galaxies, one still has to estimate the optical depth of the intergalactic medium (IGM). This section describes the prescription we use. Given the comoving emissivity of hydrogen-ionizing flux $\epsilon(\nu, z)$, the specific intensity of the background flux $J(\nu_0, z_0)$ (in $\text{erg s}^{-1} \text{ cm}^{-2} \text{ Hz}^{-1} \text{ sr}^{-1}$) is calculated using

(Bechtold et al. 1987):

$$J(\nu_0, z_0) = \frac{cH_0^{-1}}{4\pi} \int_{z_0}^{\infty} dz \frac{(1+z_0)^3}{(1+z)^5(1+\Omega_0 z)^{1/2}} \times \epsilon(\nu, z)(1+z)^3 \exp[-\tau(\nu_0, z_0, z)]. \quad (5)$$

Here $\tau(\nu_0, z_0, z)$ is the optical depth for a photon emitted at redshift z with frequency ν and observed at redshift z_0 with frequency $\nu_0 = \nu(1+z_0)/(1+z)$. In this paper we assume that this optical depth is due to H I in Lyman α system clouds encountered along any line of sight. The absorption by singly ionized helium is negligible in determining the hydrogen-ionizing flux. Neutral helium is always a subdominant species in the Lyman α clouds when the background flux is dominated by quasars or star-forming galaxies. Therefore we neglect the absorption by neutral helium. We also neglect the absorption by diffuse H I in the intergalactic medium, because there is no evidence for its presence.

The line-of-sight average optical depth $\tau_{\text{Ly}}(\nu_0, z_0, z)$ due to Poisson-distributed Lyman α clouds can be expressed as (Paresce, McKee & Bowyer 1980):

$$\tau_{\text{Ly}}(\nu_0, z_0, z) = \int_{z_0}^z \int_0^{\infty} dz dN_{\text{HI,IGM}} \mathcal{P}(N_{\text{HI,IGM}}, z) \times \{1 - \exp[-N_{\text{HI,IGM}} \sigma_{\text{HI}}(\nu)]\}. \quad (6)$$

Here $N_{\text{HI,IGM}}$ is the neutral hydrogen column density of the Lyman α clouds, and $\mathcal{P}(N_{\text{HI,IGM}}, z)$ is the average number of clouds with H I column density between $N_{\text{HI,IGM}}$ and $N_{\text{HI,IGM}} + dN_{\text{HI,IGM}}$ in a redshift range z to $z + dz$ along any line of sight. With the existing observations, it is not possible to fix uniquely the form of $\mathcal{P}(N_{\text{HI,IGM}}, z)$ from $0 \leq z \leq 4$. For $z \geq 1.7$ we take model 3 of Giroux & Shapiro (1996) for Lyman α clouds, with $N_{\text{HI}} \leq 1.5 \times 10^{17} \text{ cm}^{-2}$. For $z \leq 1.7$, we take the redshift evolution given by Bahcall et al. (1993) and normalize the number of clouds per unit redshift at $z = 1.7$ with model 3 of Giroux & Shapiro (1996). This is consistent with the findings of Bahcall et al. (1993) for clouds with equivalent width $W \geq 0.32 \text{ \AA}$ ($N_{\text{HI}} = 1.5 \times 10^{14} \text{ cm}^{-2}$). For Lyman-limit systems ($N_{\text{HI}} \geq 1.5 \times 10^{17} \text{ cm}^{-2}$), the results of Stengler-Larrea et al. (1995) are taken for $0 \leq z \leq 4$. The emissivity $\epsilon(\nu, z)$ is determined from the galaxy evolution models that fulfil a certain criterion described in the next section. The contribution of ionizing flux from ‘reprocessing’ inside Lyman α clouds is neglected in our estimates (for details see Haardt & Madau 1996).

3 RESULTS

3.1 Parameters

In the following, we consider the so-called standard cold dark matter (SCDM) model with $H_0 = 50 \text{ km s}^{-1} \text{ Mpc}^{-1}$, $\Omega_0 = 1$, $\Lambda = 0$ and $\sigma_8 = 0.67$. We take the baryonic fraction to be $\Omega_B = 0.05$, consistent with primordial nucleosynthesis. Our approach in this paper is to work within the framework of one cosmological model and a single set of values of the parameters, and to assume that all the changes that may occur from altering these choices can be compensated by appropriately adjusting the free parameters of the semi-analytic models of galaxy formation. As a matter of fact, it seems that the uncertainties from various galactic evolution processes (like interactions, mergers, etc.) are more important than the potential influence of the background cosmology and structure formation models (Heyl et al. 1995).

For simplicity, we take the Salpeter initial mass function (IMF) with index $x = 1.35$. Stars have masses $0.1 M_{\odot} \leq m \leq 120 M_{\odot}$,

and we assume that the mass fraction forming dark objects with masses below $0.1 M_{\odot}$ is negligible. Though we have used a Salpeter IMF throughout this paper, it is possible that the IMF at high redshift is top-heavy and hence produces more UV flux. We ran a few models with a top-heavy IMF at high z and noticed that we overestimate the metal production by a considerable amount. However, these models may be allowed if a large fraction of metals are blown away with galactic winds in the IGM. Present observations suggest that as much as half of the metals at high redshifts are in small column density Lyman α clouds (Songaila & Cowie 1996), so it may not be unrealistic to assume that a substantial fraction of metals are blown from galaxies. However, it can enhance the Lyman-limit flux by a factor of a few units at high redshifts, which does not affect our results significantly (see the discussion in Section 3.3).

In order to put robust bounds on the hydrogen-ionizing emissivity $\epsilon(\nu, z)$ coming from galaxies, we define two models that are representative of the uncertainties in the high- z measurement of the 1620 \AA cosmic emissivity (Madau et al. 1996; Sawicki et al. 1997): model I gives a fairly good fit of Madau et al.’s results at high redshift; model II matches values determined by Sawicki et al. Both models are completely defined by the three parameters previously mentioned. The first free parameter (the SFR efficiency parameter) $\beta(z)$ is shown in Fig. 1 for both models. Its strong evolution with redshift is necessary to reproduce the sharp decrease of the cosmic comoving emissivity observed by the CFRS but the results are not very sensitive to the shape of the function used provided the peak is located at the right position $z \approx 1.5$ and that $0.5 \leq \beta(z) \leq 200$. For instance, Fig. 1 clearly shows that, even though $\beta(z)$ evolves more strongly in model II (dashed curve) than in model I, there is no

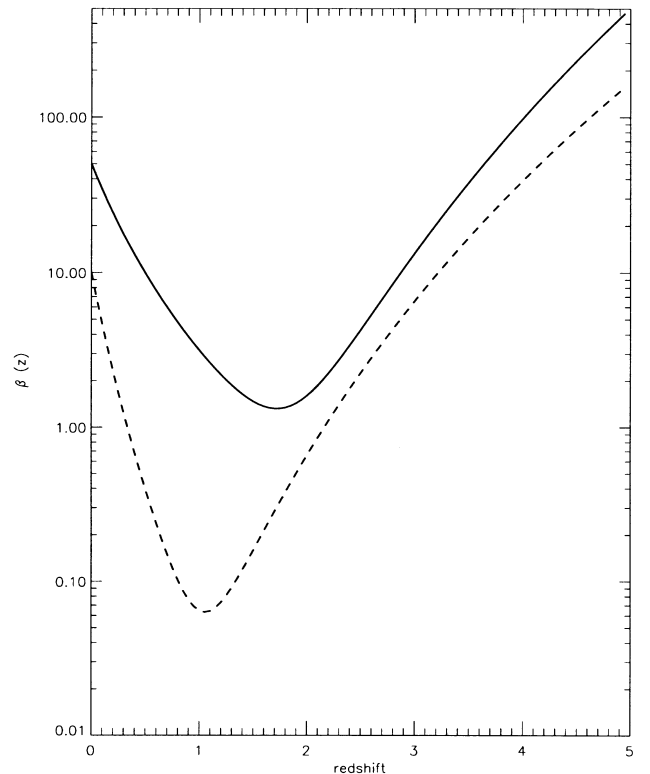


Figure 1. Efficiency parameter evolution with redshift. The solid and dashed lines show the values used for models I and II respectively. Analytical expressions for $\beta(z)$ are $\beta(z) = 50[1 + 10^{-6}(1 + z_{\text{coll}})^{13}]/(1 + z_{\text{coll}})^4$ (model I) and $\beta(z) = 10[1 + 10^{-5}(1 + z_{\text{coll}})^{16}]/(1 + z_{\text{coll}})^8$ (model II).

drastic difference in the cosmic emissivity around the peak in both models.

The value of the concentration parameter f_c is quite poorly known but, as pointed out in GHBM (their fig. 6), the prescription given above allows one to match quite well the measured FIR and millimetre emission of a flux-limited sample dominated by mild starbursts and luminous IR galaxies (Franceschini & Andreani 1995) provided one takes $f_c \approx 2.7$. However, such observations tend to pick out galaxies with central, dense regions undergoing star formation (Sanders & Mirabel 1996) and therefore are biased to give smaller values of f_c . On the other hand, as argued by Mo, Mao & White (1997) and Lobo & Guiderdoni (in preparation), semi-analytic models predict too small disc radii in the SCDM as

compared to observations. Hence, we fix the value of f_c to get the correct distribution of DLA (Fig. 2), which is based on the absorption properties of these clouds. The influence of f_c concerns mainly the H I distribution: the larger the value of this parameter, the more extended the H I exponential discs and the fewer the DLA systems. There is likely to be a redshift dependence of this parameter, simply because mergers have a well-known tendency to concentrate the gaseous content of discs. However, we did not try to model that effect, but rather took an average value of the parameter over redshift. Averaged values $f_c = 7$ for model I and $f_c = 5$ from model II allow us, as shown in Fig. 2, to reproduce quite well the column density distribution of DLA at several redshifts.

Finally, as discussed in the last section, the value of the third

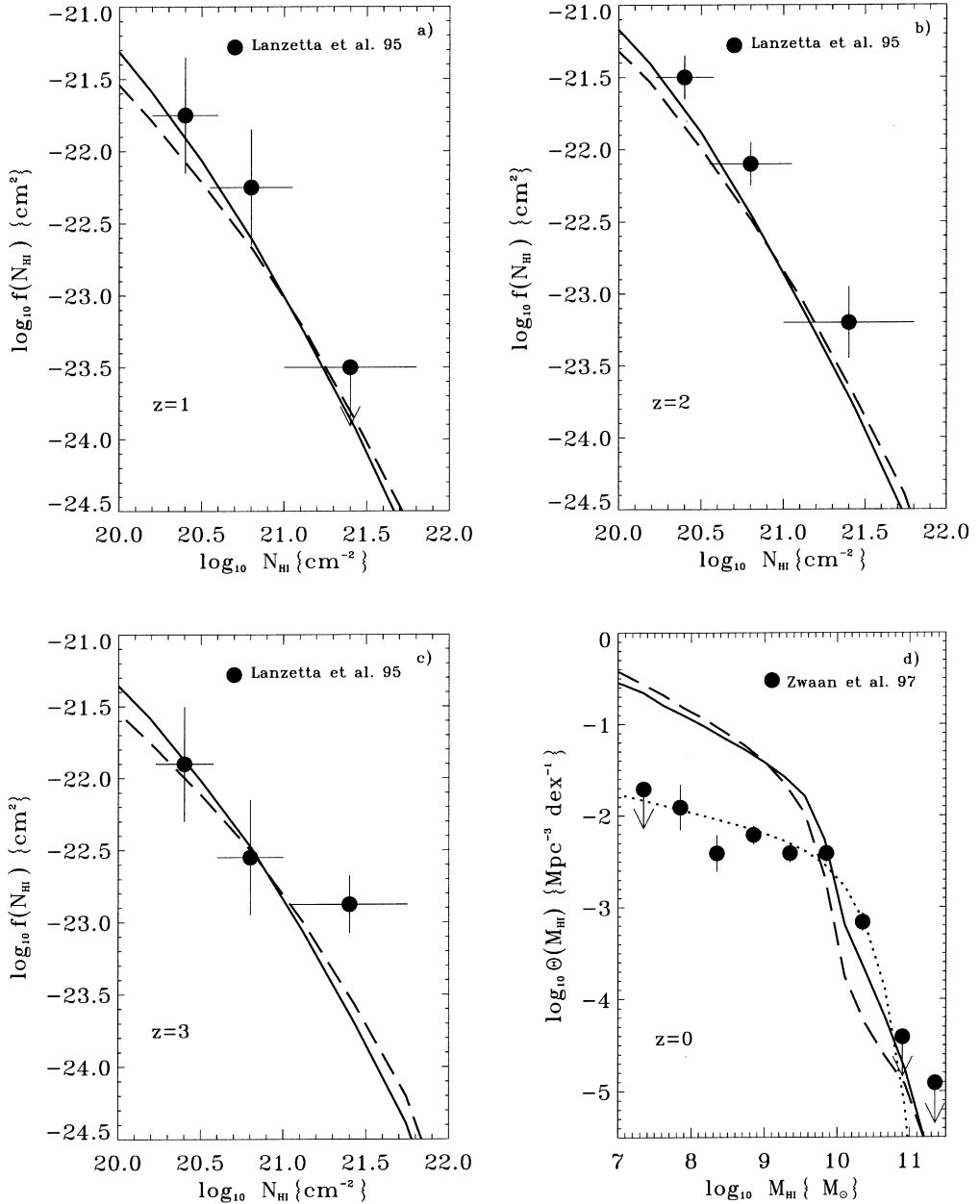


Figure 2. (a) Distribution of damped Lyman α absorbers as a function of their H I column density at $z \approx 1$. Solid and dashed lines are respectively the predictions of models I and II. (b) Same as (a) for $z \approx 2$. (c) Same as (a) for $z \approx 3$. (d) H I mass function of galaxies at $z \approx 0$. Solid, dashed and dotted curves are respectively models I and II predictions and a Schechter fit to the data given by Zwaan et al. (1997).

parameter (the feedback parameter), V_{hot} , is difficult to determine. However, it has very little influence on the results because it mainly affects the faint-end slope of the H I mass function, so we just tuned it in order to get the right amount of H I in DLA systems at high z (Storrie-Lombardi, McMahon & Irwin 1996). Such a requirement yields values for model I and II of 120 and 100 km s⁻¹ respectively.

3.2 Luminosity densities

Figs 3 and 4 show results for the two models discussed above. The ‘merit’ of a model is judged by its ability to predict correctly the evolution of emissivities in various wavebands, the evolution of Ω_{HI} and the average metallicity of DLA absorbers from $0 \approx z \leq 4$. The

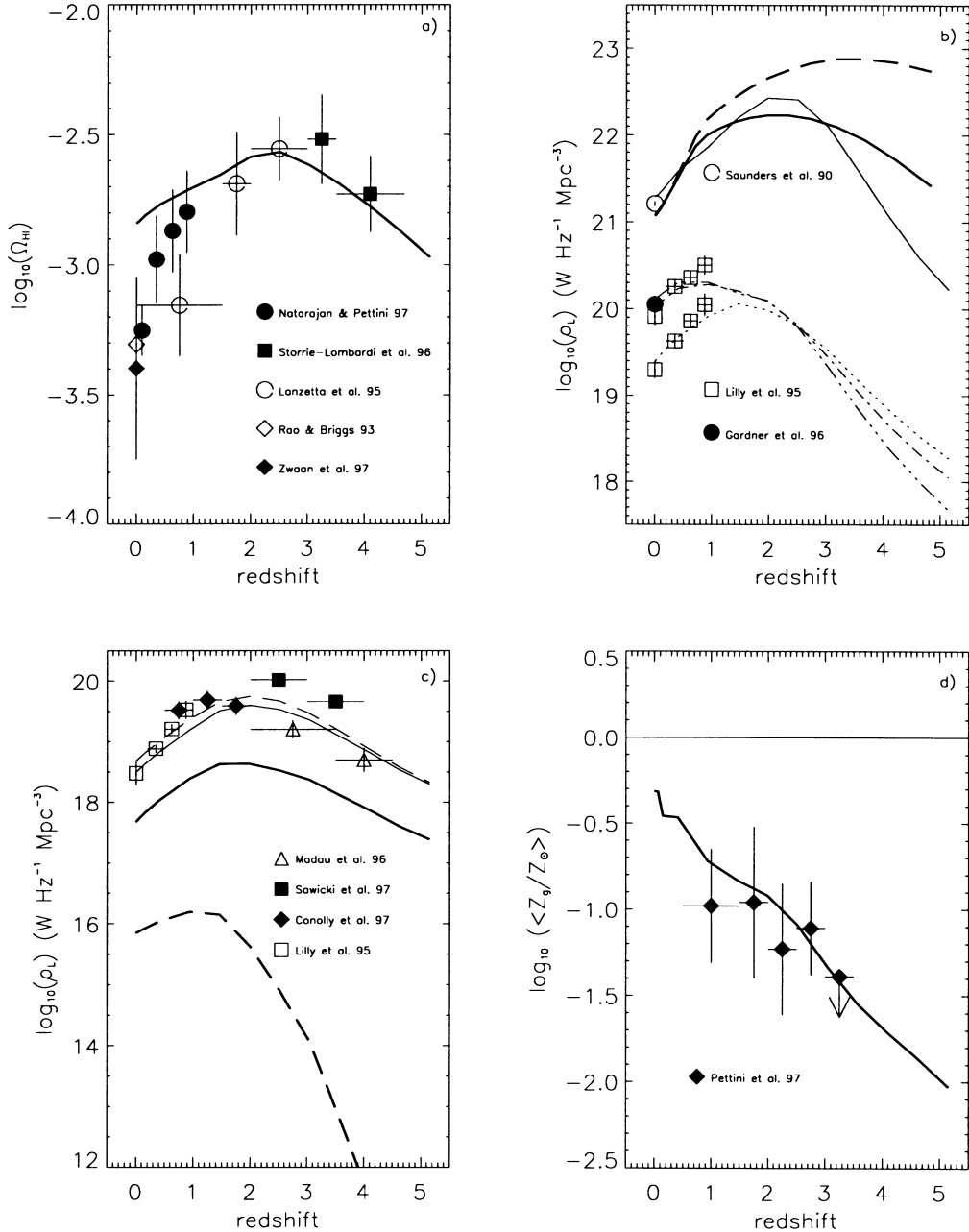


Figure 3. (a) Evolution of the cold gas density parameter in DLA absorbers. The fit from model I is indicated by the solid line. (b) Rest-frame comoving luminosity density from optical to FIR. The thin dotted, dot-dashed, triple-dot-dashed and solid lines respectively stand for emissivities at 4400 Å, 10000 Å, 22000 Å and 60 μm given by model I. Open squares: local and Canada–France Redshift Survey (Lilly et al. 1996). Open circle: 60 μm local density corresponding to one-third of the bolometric light radiated in the IR (Saunders et al. 1990). Solid circle: 2.2 μm local luminosity density (Gardner et al. 1996). The thick solid and dashed lines are respectively models (A) and (E) from GHBM that give reasonable fits of the CIB. (c) Rest-frame comoving luminosity density from far-UV to UV. The thin solid and dashed lines represent emissivities at 1620 and 2800 Å given by model I. The thick solid and dashed lines are predictions of the same model for luminosity at 912 Å respectively without and with H I absorption, but with dust absorption. Solid diamonds: photometric redshifts in the *Hubble Deep Field* (Connolly et al. 1997) taking into account NIR data. Solid squares: other estimates of photometric redshifts in the HDF (Sawicki et al. 1997). Open triangles: HDF with redshifts from Lyman-continuum drop-outs (Madau et al. 1996). (d) Evolution of the mean metallicity in damped Lyman α absorbers. Prediction from model I is indicated by the thick solid line. Since the chemical evolution model is a closed-box one, the metallicity of the systems is certainly overestimated if a fraction of the metals is ejected in the IGM.

predicted evolution of the Lyman-limit emissivities – with or without absorption by H I in the interstellar medium of galaxies – is also shown in the figures. As seen in Figs 3 and 4, the two models capture fairly well the broad features of the Universe up to $z \approx 4$. The only discrepancy between the observations and theoretical estimates is that these models predict too high a value of Ω_{HI} at $z \approx 0$ (Figs 3a and 4a). To investigate this point in detail, we show in Fig. 2 the H I mass function at $z = 0$ (Zwaan et al. 1997), along with the distribution of H I column density in DLA absorbers at three redshifts (Lanzetta et al. 1995). Although the agreement at higher redshift is seen to be quite good, the disagreement at $z = 0$ can be noticed in Fig. 2(d). Whereas the deviation of theoretical predictions from the observed H I mass function at small H I masses is probably the result of our feedback prescription, we also underestimate slightly the H I content for $10^9 M_{\odot} \leq M_{\text{HI}} \leq 5 \times 10^{10} M_{\odot}$.

The disagreement at large H I masses is more important because most of the hydrogen-ionizing photons are seen to be emitted by the largest masses in our models. Nevertheless, this discrepancy, which would result in an underestimate of the H I absorption in the ISM in evaluating the hydrogen-ionizing emissivity, is somewhat alleviated by the fact that the SFR is also lower because of its proportionality to the gas mass (equation 1).

The emissivity of Lyman-limit photons depends sensitively on dust and H I absorption in the ISM. At $z \approx 0$, the amount of dust in galaxies is fixed by matching the energy re-radiated in the FIR and millimetre bands with *IRAS* results at $60 \mu\text{m}$, as shown in Figs 3 and 4. At high redshifts, there is a greater uncertainty in the average amount of dust in galaxies. We use equation (4), which relates the dust optical depth with the average hydrogen column density $\langle N_{\text{HI,ISM}}(t) \rangle$ and metallicity $Z_g(t)$ of a galaxy, to fix the dust content

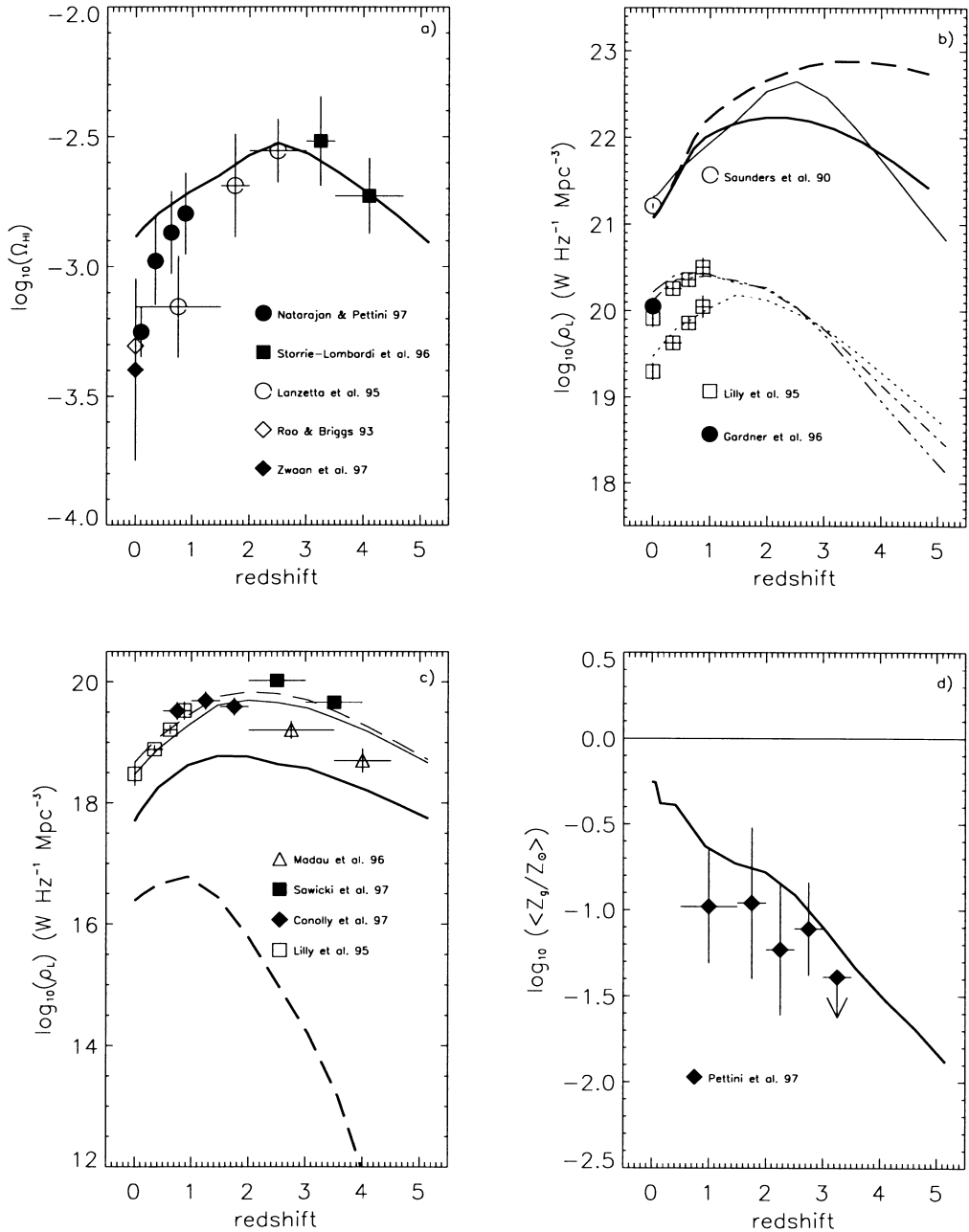


Figure 4. Same as Fig. 3 but for model II.

in a galaxy to within the observational uncertainties in the evolution of $\langle N_{\text{HI,ISM}}(t) \rangle$ and $Z_g(t)$. The recent detection of the CIB (Puget et al. 1996; Guiderdoni et al. 1997a) can also be used to constrain the history of dust emission in the Universe. GHBM used semi-analytic models of galaxy formation to explain the observed CIB. We plot the results of their models (A) and (E), which successfully explain Puget et al.'s results, in Figs 3(b) and 4(b) along with the prediction of our models at $\lambda = 60 \mu\text{m}$. It is quite clear that there is a good agreement between the two results. Therefore, we believe that our method allows us to get a fair estimate of dust absorption for $0 \leq z \leq 4$.

As is evident from Figs 3 and 4, the H I absorption in the ISM is the most important factor in determining the hydrogen-ionizing emissivity. It is customary to compute the emissivity of galaxies and multiply by a constant escape fraction to account for this uncertainty (see e.g. Giallongo et al. 1997). We model this by using equation (4) for the optical depth of the neutral hydrogen in a galaxy. As discussed above, in a geometry where the gas and stars are homogeneously mixed, it just means that a factor $1/\langle \tau_{912} \rangle$ of all the hydrogen-ionizing photons can escape from the galaxy. As $\langle \tau_{912} \rangle \gg 1$, the validity of such an assumption depends crucially on the relative distribution of stars and neutral hydrogen in the ISM. However, it should be pointed out that a homogeneous distribution gives an overestimate of the absorption, i.e. an optically thick but clumpy medium will always result in less absorption, and therefore the average emissivity that we estimate is a secure lower limit on the hydrogen-ionizing emissivity from star-forming galaxies.

3.3 Galactic background Lyman-limit flux

The evolution of the background flux of Lyman-limit photons for various cases discussed above is shown in Fig. 5 along with the

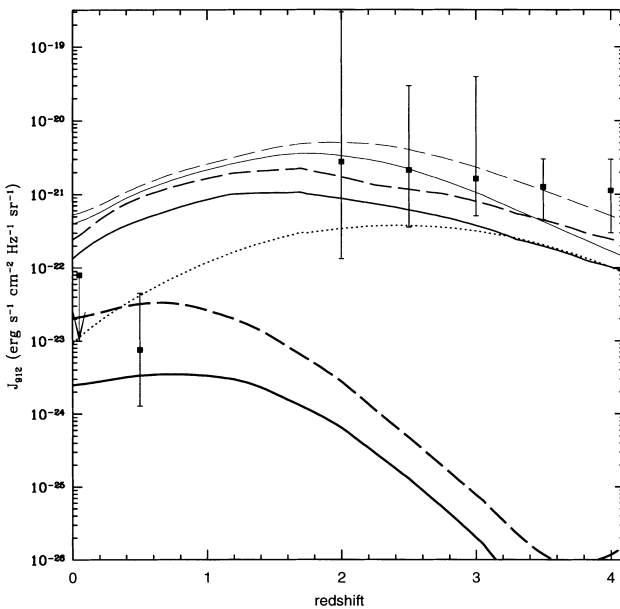


Figure 5. The evolution of Lyman-limit flux is shown for the various cases discussed in the text. The solid lines give the predictions of model I. The lines of increasing thickness correspond respectively to models without dust and H I absorption, with dust but without H I absorption, and with both dust and H I absorption. The dashed lines are the corresponding predictions of model II. The dotted line shows the evolution of background Lyman-limit flux from quasars. The upper limit at $z \approx 0$ is from Vogel et al. (1995), the data point at $z \approx 0.5$ is from Kulkarni & Fall (1993), and the high-redshift data points are from Cooke et al. (1997).

available observations at low and high redshifts. The high-redshift data shown in Fig. 5 are taken from Cooke et al. (1997). Other high-redshift proximity effect calculations such as the one by Giallongo et al. (1996) give $J_{\text{ion}} \approx (5 \pm 1) \times 10^{-22} \text{ erg s}^{-1} \text{ cm}^{-2} \text{ Hz}^{-1} \text{ sr}^{-1}$ independent of the redshift for $2 \leq z \leq 4$. The evolution of the quasar contribution is also shown, based on the quasar luminosity function derived by Pei (1995). All the observational results discussed before give the background hydrogen-ionizing flux, J_{ion} , as opposed to the Lyman-limit flux that we calculate. They are related by: $J_{\text{ion}} = 3/(3 + \delta) \times J_{912}$, where δ is the spectral index of the UV background flux (Miralda-Escudé & Ostriker 1992). For quasar and galaxy UV backgrounds, $\delta \approx 1-2$ (see e.g. Miralda-Escudé & Ostriker 1990). We scale all the values of J_{ion} assuming $\delta = 1$, at all redshifts, in Fig. 5. We also show the flux without dust absorption to gauge the relative importance of dust absorption as compared to H I absorption. It should be pointed out that the curves without dust absorption are not normalized to HDF and CFRS fluxes at other wavebands, so they cannot be taken as realistic estimates of Lyman-limit flux; their only purpose is to estimate the relative importance of dust and H I extinction of the Lyman-limit flux. As is clearly seen, dust absorption decreases the H I flux typically by a factor of a few while the H I absorption can diminish it by nearly three orders of magnitude at high redshift.

If the absorption of Lyman-limit photons by H I in the ISM of a galaxy is neglected, then the background hydrogen-ionizing flux from star-forming galaxies can be comparable to or dominate the flux from quasars and might make up for the extra flux that might be required to explain the proximity effect (Cooke et al. 1997). However, we believe that it is highly unrealistic to neglect completely the H I absorption in the ISM. As Fig. 5 shows, the ionizing flux at $z \approx 3$ decreases by more than three orders of magnitude when this absorption is taken into account. Such a decrease cannot be compensated by the uncertainties in our analysis, and therefore it seems unlikely that star-forming galaxies dominate the hydrogen-ionizing flux at high redshifts. The situation is quite different at smaller redshifts. At $z \approx 0$, even the lower limit to galactic flux (see the lower set of curves in Fig. 5) might be more than the quasar contribution. As discussed above, we overestimate the H I absorption in the ISM and so the value of the ionizing flux at $z \approx 0$ could be higher by a factor of a few over the values shown in Fig. 5. Therefore, though quasars are likely to dominate the background hydrogen-ionizing flux at high z , the substantial contribution to this flux at smaller redshift is very likely to be from star-forming galaxies. Our results are in qualitative agreement with the recent estimates of Giallongo et al. (1997) and Deharveng et al. (1997).

The nature of the ionizing background at high redshifts is also indicated by the recent observation of He II at high redshifts (see e.g. Davidsen, Kriss & Zheng 1996). These observations allow one to estimate the softness parameter, $S_L \equiv J_{912}/J_{228}$. At $z \approx 3$, $S_L \approx 40$ for quasar-dominated background flux (Haardt & Madau 1996) but can be as high as 1000 for background flux dominated by star-forming galaxies (Miralda-Escudé & Ostriker 1990). However, various uncertainties in the modelling of Lyman α clouds at high z as well as in the observations do not allow a firm conclusion on the softness of the ionizing background at high z (Sethi & Nath 1997). We also note that the recent numerical simulations of Lyman α absorbers show a good match with the observations if a low value of $J_{912} (\approx (1-4) \times 10^{-22} \text{ erg s}^{-1} \text{ cm}^{-2} \text{ Hz}^{-1} \text{ sr}^{-1})$ and a quasar-like spectrum are adopted (Miralda-Escudé et al. 1996; Zhang et al. 1996). Therefore, it seems that apart from a few estimates of the proximity effect (Cooke et al. 1997), the value of ionizing flux implied by the observed quasars may suffice to explain

other observations at high z , which is in agreement with our conclusions.

4 DISCUSSION

What are the various sources of uncertainties and errors in our estimates? We have assumed that the stars, dust and H I are homogeneously distributed in the galaxy, which, as already discussed, is not entirely justified. In this section, we discuss the possible implications of relaxing this assumption.

Throughout this paper we use equations (1) and (4), which give the SFR and optical depth averaged over the entire disc. We experimented with a few cases in which we considered the effect of *local* SFR and τ_λ . We subdivided the disc into shells of increasing radii and estimated the SFR and optical depth averaged over these shells; this enabled us to calculate the amount of Lyman-limit photons escaping from the disc as a function of the radial distance. In this case, both the SFR and the optical depth decrease towards the outer regions of the galaxy. The aim of this exercise was to investigate whether the decrease in SFR is less important than the decrease in the optical depth, and a relatively larger fraction of Lyman-limit photons could escape from outer parts of a galaxy. However, this does not happen because, for our values of f_c , the disc remains optically thick to Lyman-limit photons even at the truncation radius r_g where the H I column density $N_{\text{HI,ISM}}(r_g) = \langle N_{\text{HI,ISM}} \rangle / 1.6 f_c^2 \exp(-1.6 f_c)$, which means that even there the fraction of Lyman-limit photons that can escape remains approximately equal to $1/\tau_{912}$. As both the SFR and τ_{912} are proportional to $\langle N_{\text{HI,ISM}} \rangle$ (equations 3 and 4), the decrease in the optical depth is compensated by a similar decrease in SFR. Therefore, the total emergent flux from a galaxy remains the same whether we consider quantities averaged over the entire disc or we sum the contributions of all the shells.

Though it is extremely difficult to model accurately the clumpiness of the ISM, we give below a qualitative argument to gauge its effect on the H I ISM absorption. Let us assume that all the H I in the ISM is in the form of H I clouds with number of clouds per column density $f(N_{\text{HI,ISM}})$ distributed as

$$f(N_{\text{HI,ISM}}) \equiv \frac{d\mathcal{N}}{dN_{\text{HI,ISM}}} = AN_{\text{HI,ISM}}^{-\gamma}. \quad (7)$$

The optically thin clouds ($N_{\text{HI,ISM}} \leq \sigma_{\text{HI}}^{-1}$) mimic the homogeneous part of the ISM while the clouds with $N_{\text{HI,ISM}} \geq \sigma_{\text{HI}}^{-1}$ correspond to the clumpy ISM. The total average optical depth, along any line of sight, that results from Poisson-distributed clouds with this distribution is

$$\langle \tau_{\text{ISM}}^{\text{C}} \rangle \equiv \int_{N_{\text{HI,ISM}}(\text{min})}^{N_{\text{HI,ISM}}(\text{max})} [1 - \exp(-N_{\text{HI,ISM}} \sigma_{\text{HI}})] f(N_{\text{HI,ISM}}) dN_{\text{HI,ISM}}. \quad (8)$$

Our aim is to calculate the absorption from the clumpy part of the ISM and see what difference it would make if the same amount of matter was distributed homogeneously. To do that, we are interested in the ratio of the average optical depth of the clumpy medium from equation (8) and $\langle \tau_{\text{ISM}}^{\text{H}} \rangle \equiv \langle N_{\text{HI,ISM}} \rangle \sigma_{\text{HI}}$, the optical depth of the H I in the clumpy medium was distributed homogeneously. We further assume that the ionizing stars are located outside the clouds in order for the H I absorption to be minimum. For the distribution given by equation (7), we get

$$\frac{\langle \tau_{\text{ISM}}^{\text{C}} \rangle}{\langle \tau_{\text{ISM}}^{\text{H}} \rangle} = \frac{(-\gamma + 2) [N_{\text{HI,ISM}}^{(\gamma+1)}(\text{max}) - N_{\text{HI,ISM}}^{(\gamma+1)}(\text{min})]}{(-\gamma + 1) [N_{\text{HI,ISM}}^{(\gamma+2)}(\text{max}) - N_{\text{HI,ISM}}^{(\gamma+2)}(\text{min})]} \frac{1}{\sigma_{\text{HI}}}. \quad (9)$$

Observations of H I clouds in the ISM of our Galaxy suggest that the clouds have a distribution given by equation (7) with $1.6 \leq \gamma \leq 2.2$ for 10^{18} at $\text{cm}^{-2} \leq N_{\text{HI,ISM}} \leq 10^{22}$ at cm^{-2} (Dickey & Garwood 1990), which corresponds to the clumpy part of the ISM. For these values, $0.01 \leq \langle \tau_{\text{ISM}}^{\text{C}} \rangle / \langle \tau_{\text{ISM}}^{\text{H}} \rangle \leq 0.03$ [$\gamma = 2$ is excluded as equation (9) is not valid for this value]. Our simple analysis suggests that the average optical depth from the clumpy part of the ISM is negligible as compared to the homogeneous part; and much of the absorption is caused by the fraction of H I in the homogeneous medium (or optically thin clouds) in the ISM. There is a great amount of uncertainty in determining the fraction of the homogeneously distributed H I in the ISM. If, for the purpose of this paper, we roughly assume that the H I is distributed equally between the homogeneous and the clumpy ISM, as might be the case for our Galaxy, then our analysis suggests that the average optical depth of the ISM is halved as compared to the case when the entire ISM is made up of homogeneously distributed H I.

It is known that a significant fraction of young stars form inside optically thick clouds, which suggests that the arguments given above underestimate the absorption. On the other hand, most of the ionizing stars form in OB associations. The UV photons from these stars could puncture the layer of neutral hydrogen to escape into the galactic halo. This fact can be used to explain the existence of H II at large scaleheights (Reynolds 1984), which requires a large fraction of the photons to escape in the halo (Dove & Shull 1994). However, it is not clear what fraction of this ionizing flux can escape the halo of a galaxy. The observational status of hydrogen-ionizing flux from other galaxies is uncertain. Recent observation of four low-redshift starburst galaxies (Leitherer et al. 1995) allows one to get only upper limits of 57, 5.2, 11.3 and 3.2 per cent on the escape fraction (Hurwitz, Jelinsky & Van Dyke Dixon 1997). Other arguments based on H α luminosity density of the Universe give a more stringent upper limit of ~ 1 per cent on the escape fraction (Deharveng et al. 1997). We note that our simple assumption, without puncturing, already gives an average escape fraction of 0.4–1 per cent at small redshifts, which is within the observational uncertainties. Therefore, this effect seems unlikely to be more than a few per cent at low redshift. However, at high z , as the SFR is higher, it might well be that the puncturing effect allows a larger fraction of ionizing photons to escape.

Throughout this paper we assumed that the damped Lyman α systems are progenitors of present-day galaxies. This assumption has recently been questioned by Prochaska & Wolfe (1997). They studied the kinematical properties of damped Lyman α systems at high redshift and concluded that most damped Lyman α systems correspond to thick rotating discs with rotational velocities ≈ 225 km s^{-1} . We compare these results with the predictions of our model. We notice that for the SCDM model, even though about 10 per cent of the objects have rotational velocities beyond the value of ≈ 225 km s^{-1} , the average rotational velocity of damped Lyman α systems is 120 km s^{-1} at $z \approx 3$, which is too small to be consistent with Prochaska & Wolfe's (1997) results. However, this discrepancy is not serious, for various reasons. First, the relationship between rotational velocity and N_{HI} depends sensitively on the cosmology. We tried a structure formation model with an open universe that has $\Omega = 0.3$. In this case, the average rotational velocity increases to 160 km s^{-1} with more than one-quarter of the objects with velocities greater than ≈ 225 km s^{-1} . This increase is not unexpected because, in open universes, structures of galaxy sizes collapse at higher redshifts as compared to flat cosmology. Secondly, the distribution of rotational velocities for damped Lyman α systems depends crucially on the feedback. An increase

in feedback parameter V_{hot} results in an increase in the average rotational velocity by cutting off contributions from smaller systems. Such an increase in the feedback might come either from local uncertainties in feedback (equation 2) or from a global process like a hot IGM with temperature $T \approx 10^6$ K at high redshifts and therefore would depend on the thermal history of the IGM. We also compared the distribution of impact parameters in our models with the inference of Prochaska & Wolfe (1997) and found good agreement from both cosmogonies. Also, other recent analyses suggest that the evidence of damped Lyman α systems being thick rotating discs is not compelling (Ledoux, Petitjean & Bergeron 1997; Ledoux et al. 1998). These authors studied the kinematical properties of a sample with 26 damped Lyman α systems and concluded that, whereas velocities up to 120 km s^{-1} might correspond to rotations of individual systems, higher velocities probably involve more than one component (Ledoux et al. 1997, 1998). A similar conclusion, based on simulations, was reached by Haehnelt et al. (1997). Therefore, it seems that, though the recent studies have thrown light on the nature of damped Lyman α systems at high z , it is still too early to draw firm conclusions. However, should it turn out that damped Lyman α systems at high z correspond to merging protogalactic H I clumps rather than rotating discs, our conclusions about the H I absorption inside the ISM of a high- z galaxy and consequently the hydrogen-ionizing flux will be significantly weakened in the sense that it will be more difficult to support the view that sites where a high H I column density is detected also correspond to star-forming regions.

5 CONCLUSION

We estimated the contribution of star-forming galaxies to the background Lyman-limit flux taking into account the H I and dust absorption in the ISM of individual galaxies in a self-consistent way with the cosmic star-formation history. We assumed that DLA systems correspond to star-forming regions at high redshift. We conclude that, while star-forming galaxies are unlikely to dominate the background hydrogen-ionizing flux at high redshift, they are most likely to do so in the present Universe. The current uncertainties of modelling do not allow us to calculate the redshift of cross-over from quasar-dominated to galaxy-dominated background flux. As already discussed, a good discriminator between these two sources of ionizing background is the softness of their spectra. Future high-resolution observations of metals (e.g. carbon) in their various ionization states in the low column density Lyman α clouds for $0 \approx z \leq 4$ might enable one to find the transition from quasar-dominated to galaxy-dominated background flux.

ACKNOWLEDGMENTS

We are pleased to thank Patrick Petitjean, R. Srianand and the anonymous referee for pertinent comments on the kinematics of DLAs.

REFERENCES

Andreani P., Franceschini A., 1996, MNRAS, 283, 85
 Bahcall J. N. et al., 1993, ApJS, 87, 1
 Bajtlik S., Duncan R. C., Ostriker J. P., 1988, ApJ, 327, 570
 Bardeen J. M., Bond J. R., Kaiser N., Szalay A. S., 1986, ApJ, 304, 15
 Bechtold J., 1994, ApJS, 91, 1
 Bechtold J., Weymann R. J., Lin Z., Malkan M. A., 1987, ApJ, 315, 180
 Blanchard A., Valls-Gabaud D., Mamon G., 1992, A&A, 264, 365

Cole S., Aragón-Salamanca A., Frenk C. S., Navarro J. F., Zepf S. E., 1994, MNRAS, 271, 781
 Connolly A. J., Szalay A. S., Dickinson M., Subbarao M. U., Brunner R. J., 1997, ApJ, 486, L11
 Cooke A. J., Espey B., Carswell R. F., 1997, MNRAS, 284, 552
 Davidsen A. F., Kriss G. A., Zheng W., 1996, Nat, 380, 47
 Deharveng J.-M., Faisse S., Milliard B., Le Brun V., 1997, A&A, 325, 1259
 Dekel A., Silk J., 1986, ApJ, 303, 39
 Désert F. X., Boulanger F., Puget J. L., 1990, A&A, 237, 215
 Dickey J., Garwood E., 1990, ApJ, 341, 201
 Dove J. B., Shull M., 1994, ApJ, 430, 222
 Dwek E., Városi F., 1996, in Dwek E., ed., AIP Conf. Proc. 348, Unveiling the Cosmic Infrared Background. Am. Inst. Phys., New York
 Efstathiou G., 1992, MNRAS, 256, 43p
 Fall S. M., Efstathiou G., 1980, MNRAS, 193, 189
 Fall S. M., Charlot S., Pei Y. C., 1996, ApJ, 464, L43
 Franceschini A., Andreani P., 1995, ApJ, 440, L5
 Franceschini A., Toffolatti L., Mazzei P., Danese L., De Zotti G., 1991, ApJS, 89, 285
 Franceschini A., Mazzei P., De Zotti G., Danese L., 1994, ApJ, 427, 140
 Frenk C. S., Baugh C. M., Cole S., Lacey G. G., 1996, in Persic M., Salucci P., eds, Dark Matter 1996: Dark and Visible Matter in Galaxies and Cosmological Implications. Sesto Pusteria. Italy
 Gardner J. P., Sharples R. M., Cannasco B. E., Frenk C. S., 1996, MNRAS, 282, L1
 Giallongo E., D'Odorico S., Fontana A., McMahon R. G., Savaglio S., Cristiani S., Molaro P., Traverso D., 1994, ApJ, 425, L1
 Giallongo E., Cristiani S., D'Odorico S., Fontana A., Savaglio S., 1996, ApJ, 466, 46
 Giallongo E., Fontana A., Madau P., 1997, MNRAS, 289, 629
 Giroux M. L., Shapiro P., 1996, ApJS, 102, 191
 Guiderdoni B., Rocca-Volmerange B., 1987, A&A, 186, 1
 Guiderdoni B., Bouchet F. R., Puget J. L., Lagache G., Hivon E., 1997, Nat, 390, 257
 Guiderdoni B., Hivon E., Bouchet F. R., Maffei B., 1998, MNRAS, 295, 877
 Gunn J. E., Peterson B. A., 1965, ApJ, 142, 1633
 Haardt F., Madau P., 1996, ApJ, 461, 20
 Haehnelt M. G., Steinmetz M., Rauch M., 1998, ApJ, 495, 647
 Heyl J., Cole S., Frenk C. S., Navarro J. F., 1995, MNRAS, 274, 755
 Hurwitz M., Jelinsky P., Van Dyke Dixon W., 1997, ApJ, 481, L31
 Kauffmann G. A. M., White S. D. M., Guiderdoni B., 1993, MNRAS, 264, 201
 Kennicutt R. C., 1989, ApJ, 344, 685
 Kennicutt R. C., 1997, in Guiderdoni B., Kembhavi A., eds, Starbursts: Triggers, Nature and Evolution. Editions de Physique, Paris, Springer-Verlag, Berlin
 Kennicutt R. C., Tamblyn P., Congdon C. W., 1994, ApJ, 435, 22
 Kulkarni V. P., Fall S. M., 1993, ApJ, 413, L63
 Lacey C., Silk J., 1991, ApJ, 381, 14
 Lacey C., Guiderdoni B., Rocca-Volmerange B., Silk J., 1993, ApJ, 402, 15
 Lanzetta K. M., Wolfe A. M., Turndale D. A., 1995, ApJ, 430, 435
 Ledoux C., Petitjean P., Bergeron J., 1997, in Petitjean P., Charlot S., eds, Structure and Evolution of the Intergalactic Medium from QSO Absorption Line Systems. IAP, Paris
 Ledoux C., Petitjean P., Bergeron J., Wampler E. J., Srianand R., 1998, submitted
 Leitherer C., Ferguson H. C., Heckman T. M., Lowenthal J. D., 1995, ApJ, 454, L19
 Lilly S. J., Tresse L., Hammer F., Crampton D., Le Fèvre O., 1995, ApJ, 455, 108
 Lilly S. J., Le Fèvre O., Hammer F., Crampton D., 1996, ApJ, 460, L1
 Madau P., 1992, ApJ, 389, L1
 Madau P., 1997a, International Origins Conference, Estes Park, CO, in press
 Madau P., 1997b, in Holt S. S., Mundy G. L., eds, Star Formation Near and Far. AIP, New York, p. 481
 Madau P., Ferguson H. C., Dickinson M. E., Giavalisco M., Steidel C. C., Fruchter A., 1996, MNRAS, 283, 1388
 Maffei B., 1994, PhD dissertation, Univ. Paris VII

- Maloney P., 1993, *ApJ*, 414, 41
Mathis J. S., Mezger P. G., Panagia N., 1983, *A&A*, 128, 212
Miralda-Escudé J., Ostriker J. P., 1990, *ApJ*, 350, 1
Miralda-Escudé J., Ostriker J. P., 1992, *ApJ*, 392, 15
Miralde-Escudé J., Cen R., Ostriker J. P., Rauch M., 1996, *ApJ*, 471, 582
Mo H. J., Mao S., White S. D. M., 1998, *MNRAS*, 295, 319
Natarajan P., Pettini M., 1997, *MNRAS*, 291, L28
Paresce F., McKee C. F., Bowyer S., 1980, *ApJ*, 240, 387
Peebles P. J. E., *The Large-Scale Structure of the Universe*. Princeton Univ. Press, Princeton NJ
Pei Y. C., 1995, *ApJ*, 438, 623
Pettini M., Smith L. J., King D. L., Hunstead R. W., 1997, *ApJ*, 486, 665
Prochaska J., Wolfe A., 1997, *ApJ*, 487, 73
Puget J. L., Abergel A., Boulanger F., Bernard J. P., Burton W. B. et al., 1996, *A&A*, 308, L5
Rao S., Briggs F., 1993, *ApJ*, 419, 515
Reynolds R. J., 1984, *ApJ*, 282, 191
Reynolds R. J., Tufté S. L., Kung D. T., MacCullough P. R., Heiles C., 1995, *ApJ*, 448, 715
Sanders D. B., Mirabel I. F., 1996, *ARA&A*, 34, 749
Saunders W., Rowan-Robinson M., Lawrence A., Efstathiou G., Kaiser N., Ellis R. S., Frenk C. S., 1990, *MNRAS*, 242, 318
Sawicki M. J., Lin H., Yee H. K. C., 1997, *AJ*, 113, 1
Sethi S., Nath B. B., 1997, *MNRAS*, 289, 634
Soifer B. T., Neugebauer G., 1991, *AJ*, 101, 354
Songaila A., Cowie L. L., 1996, *AJ*, 112, 335
Songaila A., Cowie L. L., Lilly S. J., 1990, *ApJ*, 348, 371
Steidel C. C., Giavalisco M., Pettini M., Dickinson M., Adelberger K. L., 1996, *ApJ*, 462, L17
Stengler-Larrea E. A. et al., 1995, *ApJ*, 444, 64
Storrie-Lombardi L. J., McMahon R. G., Irwin M. J., 1996, *MNRAS*, 283, L79
Vogel S., Weymann R., Rauch M., Hamilton T., 1995, *ApJ*, 441, 162
Zhang Y., Anninos P., Norman M. L., Meiksin A., 1997, *ApJ*, 485, 496
Zwaan M. A., Briggs F. H., Sprayberry D., Sorar E., 1997, *ApJ*, 490, 173